Supplementary information for

Photostable Platinated Bacteriochlorins as Potent Photodynamic Agents

Ngoc An Le[1], Vipin Babu[1], Martina Kalt[1], Lukas Schneider[1], Frank Schumer[1], Bernhard Spingler*[1]

[1] Department of Chemistry, University of Zurich, 8057 Zurich, Switzerland;

Corresponding author email address: spingler@chem.uzh.ch

S1. Synthesis of (2,6-difluorophenyl)dipyrromethane (**2**): S2
S2. Table S1. Reaction conditions for the synthesis of porphyrin **4**. S3
S3. Photophysical Studies S3
S4. Irradiation Setup for Cell Experiments S15
S5. Photocytotoxicity S15
S6. Cellular Localization S16
S7. Mitochondrion membrane dysfunction imaging S20
S8. Detection of Intracellular ROS Levels S20
S9. Table S2. Phototoxic properties of Bacteriochlorins against HeLa cells in the literature. S22
S10. Table S3. Phototoxic properties of Chlorins against HeLa cells in the literature S23
S11. Table S4. Light-dose dependence of the bacteriochlorins in HeLa cells. S25
S12. NMR spectra S26
REFERENCES S32

S1. Synthesis of (2,6-difluorophenyl)dipyrromethane[1,2] (2):

Boron trifluoride etherate (66 µL, 0.5 mmol) was added to a solution of freshly distilled pyrrole (17 mL, 0.24 mol) and 2,6-difluorobenzaldehyde (**1**) (1.4 g, 10 mmol) in DCM (20 mL). The reaction mixture was stirred at room temperature for 1 h. DCM and excess pyrrole was evaporated, and the crude product was purified by column chromatography on silica gel with hexane/DCM (2:1, v/v) as eluent, yielding product (**2**) as a white solid (1.5 g, 60%). Crystals of **2** were obtained from a super-saturated solution during column chromatography. ^{1}H-NMR (400 MHz, DMF-d$_7$): δ = 8.01 (bs, 2H), 7.17–7.05 (m, 1H), 6.80 (t, J = 9.0 Hz, 2H), 6.57 (q, J = 2.4 Hz, 2H), 6.05 (q, J = 2.9 Hz, 2H), 5.93 (d, J = 3.4 Hz, 2H), 5.80 (s, 1H). ^{19}F-NMR (376 MHz, DMF-d$_7$) δ = -113.44 (s, 2F). (+)-HRMS (ESI): *m/z* $[M+H]^+$ calcd. for $C_{15}H_{13}F_2N_2$: 259.10413 found: 259.10415.

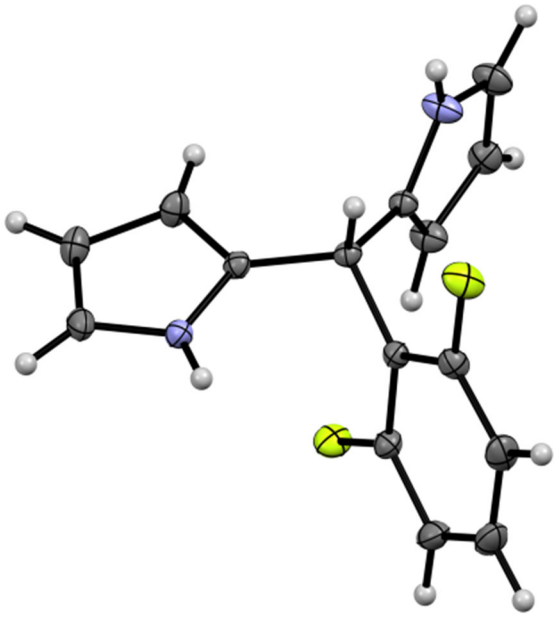

Figure S1. Displacement ellipsoid representation of the crystal structure of **2** at 50% probability.

S2. Table S1. Reaction conditions for the synthesis of porphyrin 4.

Catalyst	Concentration of catalyst [mM]	Solvent	Time [min.]	Yield
TFA	40	DCM	20	1%
TFA	81	DCM	20	3%
TFA	122	DCM	20	5%
TFA	163	DCM	20	8%
TFA	204	DCM	20	3%
TFA	163	MeOH	20	No product
TFA	163	ACN	20	No product
$BF_3 \cdot OEt_2$	40	DCM	20	20% (scrambling)
$BF_3 \cdot OEt_2$	81	DCM	20	15% (scrambling)
$BF_3 \cdot OEt_2$	122	DCM	20	12% (scrambling)

S3. Photophysical Studies

UV-Vis absorption spectra were recorded in quartz cuvettes (10 μM in DMF) on a Specord 250 plus spectrophotometer (Analytik Jena).

Fluorescence spectra were recorded on a luminescence spectrometer LS50B (Perkin Elmer) with excitation wavelength 355 nm, concentrations of BChls were 0.5 μM in MeOH.

Fluorescence quantum yields were recorded on the same spectrometer using a comparative method with anthracene in ethanol as standard ($\Phi_F = 0.27$)[3].

Equation for the calculation of the Φ_F[4]:

$$\Phi_{F(x)} = \Phi_{F(st)} \times \frac{S_x \times n_x^2}{S_{st} \times n_{st}^2} \qquad (1)$$

Where Φ_F is the fluorescence quantum yield, x and st denote compound and standard being tested, S is the slope from the plot of integrated fluorescence intensity *vs* absorbance, n and n_{st} are refractive indices of the solvents used for the samples and the standard. The absorbance of the solutions at the excitation wavelength (355 nm for all solutions) was in the range between 0.02 and 0.08.

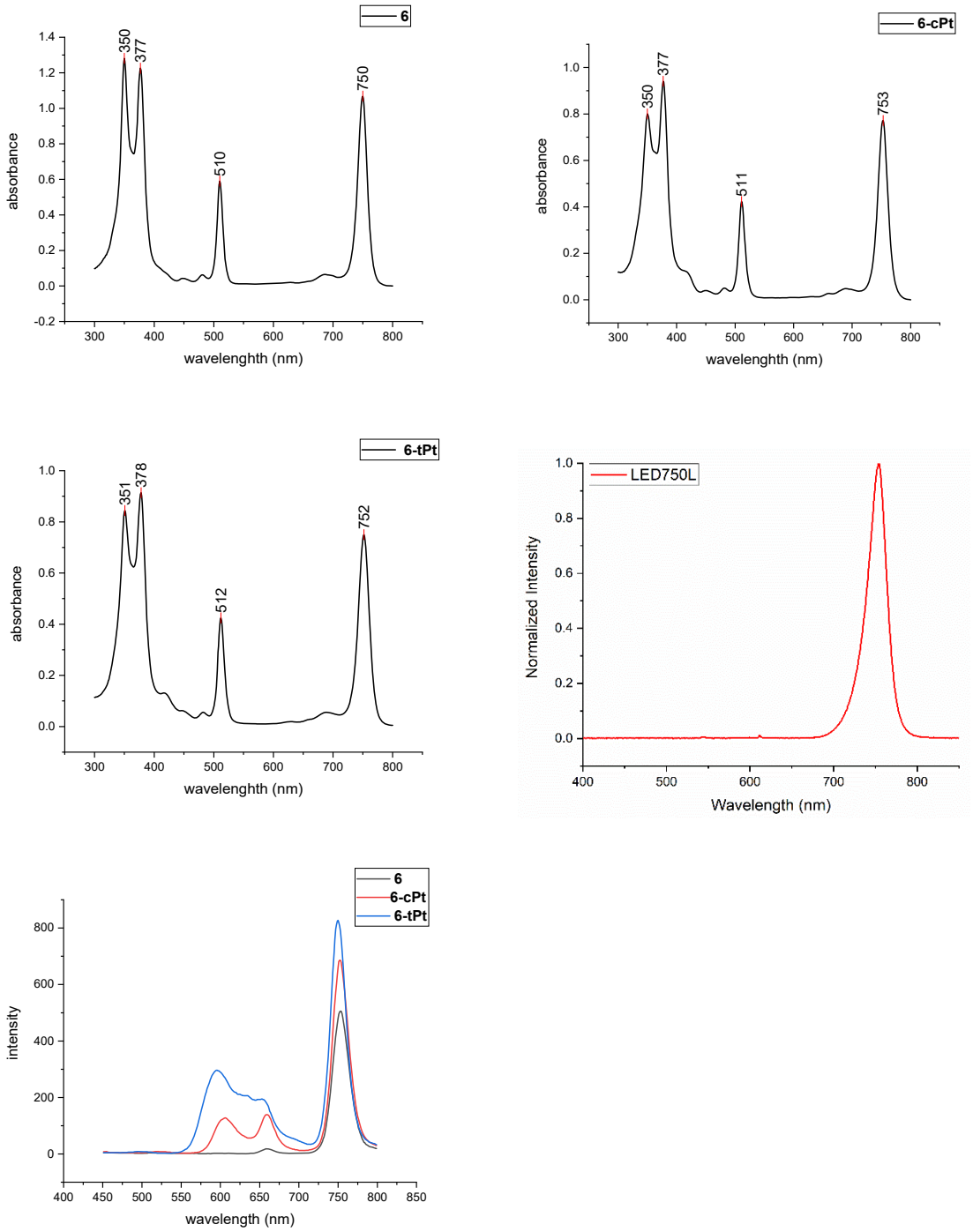

Figure S2. UV-Vis absorption of bacteriochlorins **6**, **6-cPt** and **6-tPt** (10 µM in DMF), LED emission spectrum of the LED750L used for the cell experiments, and luminescence spectra of bacteriochlorins **6**, **6-cPt** and **6-tPt** recorded (0.5 µM) in MeOH. Samples were excited at 355 nm.

Singlet oxygen quantum yields - direct method

The direct method for detection of singlet oxygen quantum yield was described by our group previously[5], using a custom-built setup as described in Figure S3. The solution of a photosensitizer in MeOH-d_4 was added in a glass cuvette (114F-10-40, 10 mm × 4 mm dimensions, Hellma Analytics, Germany). Afterwards, the cuvettes containing the samples were placed in a CUV-UV/VIS-TC-ABS temperature-controlled Qpod cuvette holder (Avantes, Netherlands). Temperature was controlled at 20 °C by a TC-125 controller (Quantum Northwest, USA) and Q-Blue software. The samples were irradiated with fiber coupled high-power LED (Prizmatix, Israel) 630 nm for MB and LED 760 nm for BChls. The light source was connected with an optical fibre (1000 µm core diameter, Avantes) to the cuvette holder over a SMA 905 fibre optic connector. The excitation power was measured to be 10.0 mW/cm^2 at the position of the cuvette using a S310C thermal sensor connected to a PM100USB power meter (Thorlabs, USA). The connection piece used to insert the SMA connector into the cuvette holder was replaced by an in-house custom-built connection piece that allows the fibre to be inserted at a distance of 2.0 cm from the cuvette. The detector (AvaSpecNIR256-1.7TEC, Avantes) was set to 0 °C and connected to the cuvette holder with an optical fibre (600 µm diameter, Avantes). Emission spectra were collected at a 90° angle with respect to the excitation beam from 1100 nm to 1400 nm after three measurement runs; every measurement run consisted of five averaged measurements each lasting 9 s. All spectra were recorded using AvaSoft 8.9 software from Avantes and further processed using Microsoft Office Excel and Origin 2019 software.

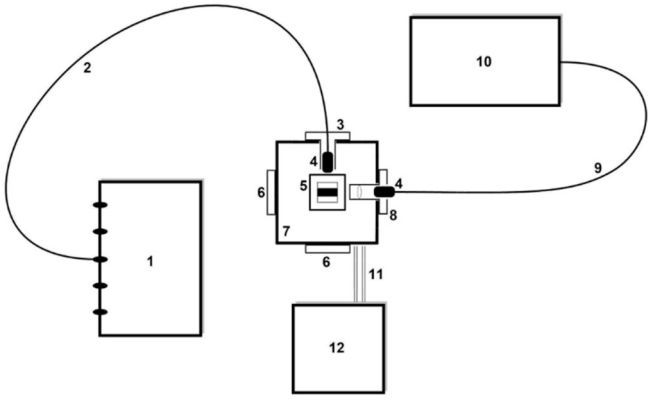

Figure S3: Setup used for NIR emission spectroscopy. **1**) high-power Multi-Wavelength Fiber-Coupled LED system FC5-LED-WL (Prizmatix), **2**) optical fibre (1000 µm). **3**) custom-built connection piece, **4**) SMA 905 fibre optic connector, **5**) cuvette in cuvette holder, **6**) blank, **7**)

temperature-controlled Qpod cuvette holder, **8**) connection piece with QIL-UV AR-coated fused-silica imaging lens, **9**) optical fibre (600 µm), **10**) NIR detector (AvaSpecNIR256-1.7TEC, Avantes), **11**) plastic hose, **12**) cooling bath. Reproduced from Ref. [5] with permission from the European Society for Photobiology, the European Photochemistry Association, and the Royal Society of Chemistry.

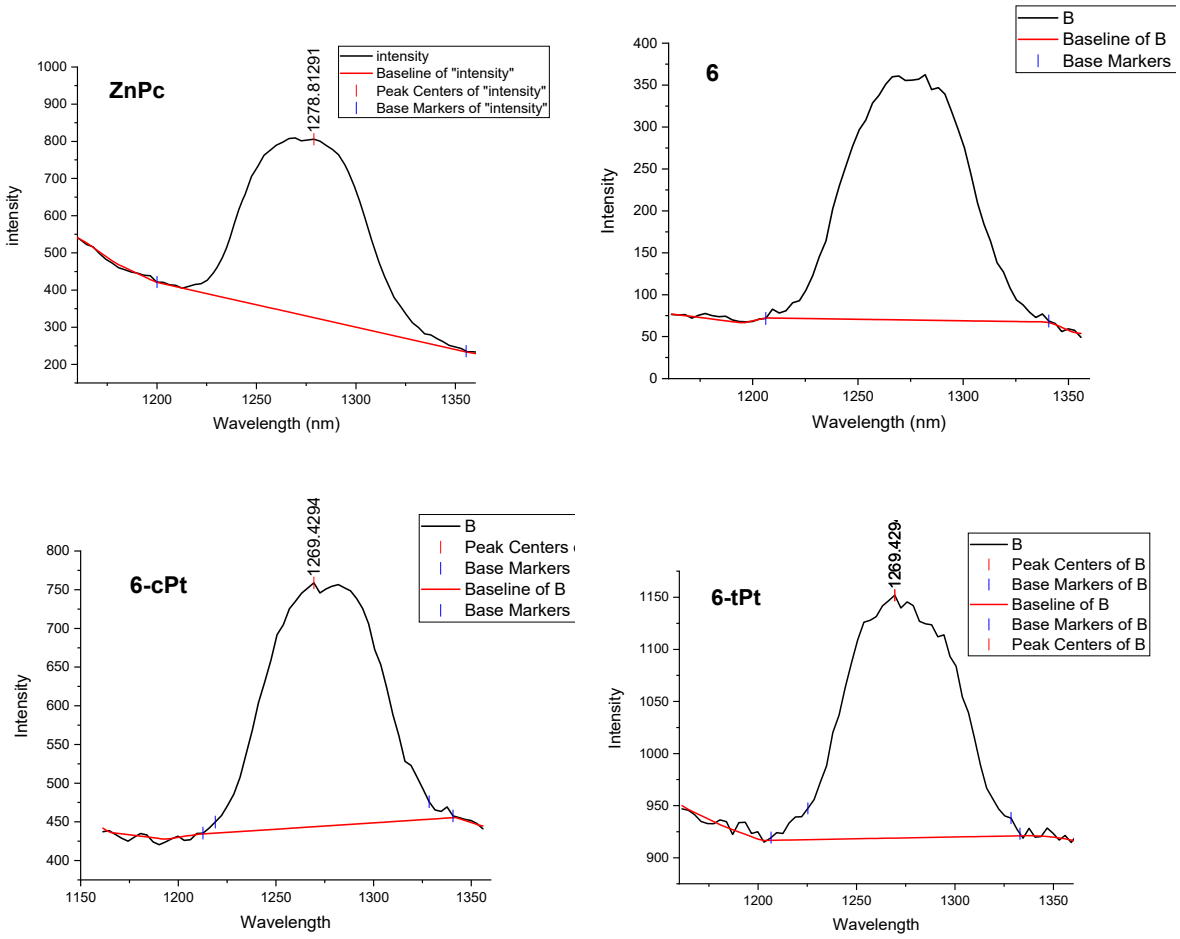

Figure S4. Typical singlet oxygen phosphorescence emission intensity in MeOH-d_4, concentration was optimised individually so that absorption lies between the range 0.05-0.1 at 760 nm for BChls and 690 nm for ZnPc.

Formula for calculation of singlet oxygen quantum yield:

$$\Phi_{\Delta(x)} = \Phi_{\Delta(st)} \times \frac{S_x}{S_{st}} \qquad (2)$$

Where Φ_Δ is the fluorescence quantum yield, x and st denote compound and standard being tested, S is the slope from the plot of area under emission spectra *vs* I, and I is the rate of light absorption calculated as overlap of the LED irradiance spectra and the absorption spectra of the compound according to the following formula:

$$I = \int I_{(\lambda)} \times [1 - 10^{-A_{(\lambda)}}] d\lambda \qquad (3)$$

Where $I_{(\lambda)}$ and $A_{(\lambda)}$ are light-flux intensity of the light source and the absorbance of the compound. Irradiance spectra of the LED light sources (Figure S5) were measured with an Avantes spectrometer AvaSpec-ULS2048CL-EVO-RS using an integration sphere, after calibration of spectrometer according to the standard procedure provided by Avantes.

For each compound, emission spectra were recorded at two different concentrations with absorption intensities in the range of 0.05 to 0.1 at 760 nm for BChls or at 630 nm for MB (4 mm light path). The slope S was calculated through the coordinates (0,0) using Origin 2019.

Singlet oxygen quantum yields - indirect method

Singlet oxygen quantum yields (Φ_Δ) of BChls were determined analogously to a method reported by Tian et al.[6] The solutions of PSs (5 μM, MeOH) and DPBF (30 μM) were placed in the cuvette holder with temperature constantly controlled at 20 °C. The LED light sources with wavelengths of 760 nm and LED 630 nm were used to irradiate BChls and MB respectively (the same light source system, cuvette holder with temperature control as describe above) (Figure S3); the metallic slit with radius 1 mm was placed in the cuvette holder **5** to adjust the light intensity and obtain reasonable decay rate of DPBF. UV-Vis spectra were recorded after every 10 seconds of irradiation showing the decrease in absorption at 415 nm. Plot the absorption at 415 nm vs time and the slopes were calculated using Origin 2019 (Fig. S6). Singlet oxygen quantum yields (Φ_Δ) were calculated using this formula:

$$\Phi_{\Delta(x)} = \Phi_{\Delta(st)} \times \frac{S_x \times I_{st}}{S_{st} \times I_x} \qquad (4)$$

Where Φ_Δ is the fluorescence quantum yield, x and st denote compound and standard being tested, S is the slope from the plot of absorption at 415 nm *vs* time, I is the rate of light absorption calculated as overlap of the LED irradiance spectra and the absorption spectra of the compound according to equation (3).

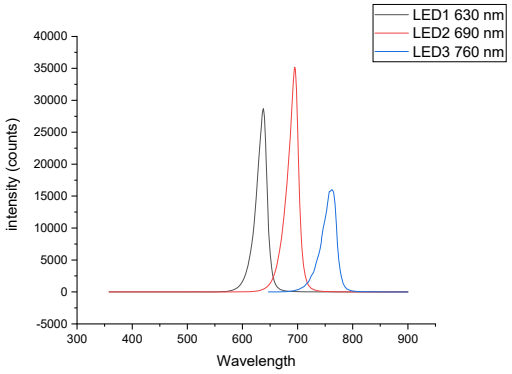

Figure S5: Irradiance spectra of high-power Multi-Wavelength Fiber-Coupled LED light sources, measured with an Avast spectrometer AvaSpec-ULS2048CL-EVO-RS using an integration sphere, spectra were measured according to standard procedure from Avantes.

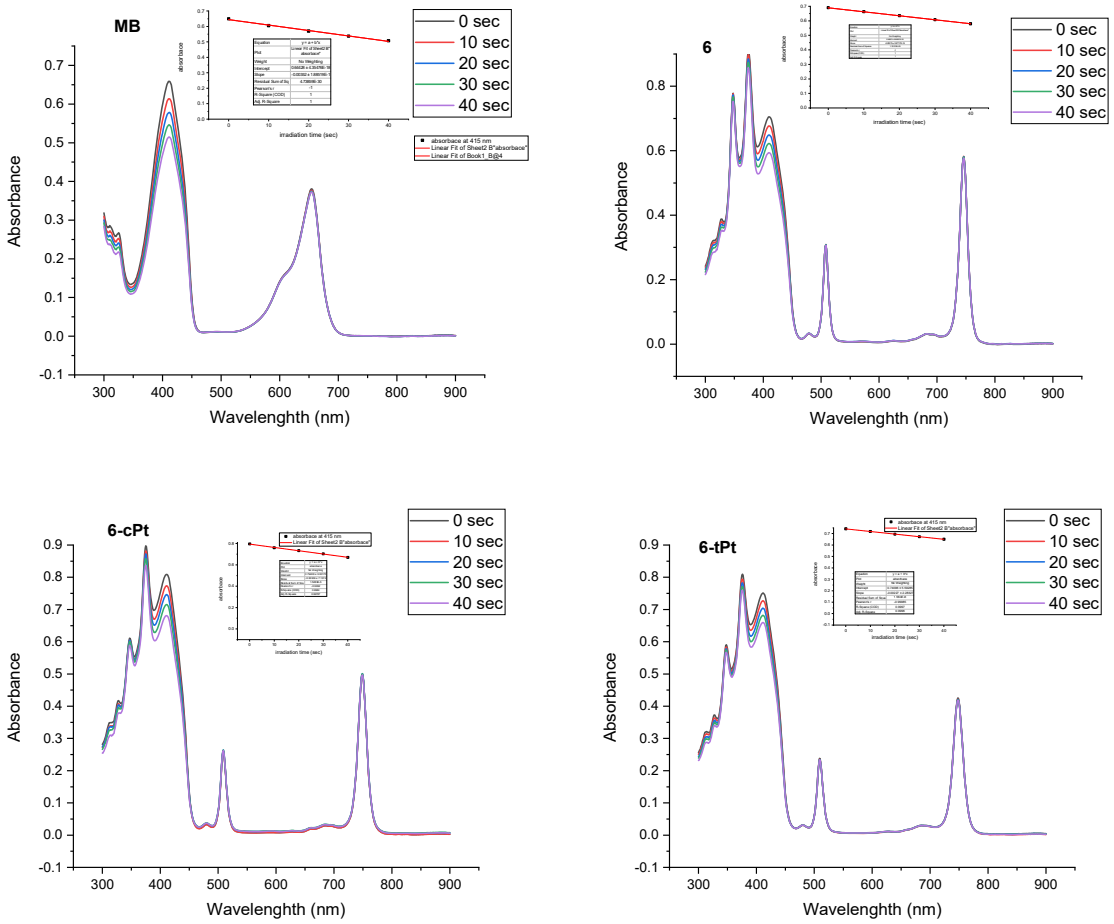

Figure S6. Determination of singlet oxygen quantum yield of BChls **6**, **6-cPt** and **6-tPt** in MeOH using DPBF (30 μM) as a singlet oxygen quencher, standard MB. Concentration = 5×10^{-6} M. (Inset: plots of DPBF absorbance at 415 nm vs. time).

Generation and detection of hydroxyl radicals (˙OH) upon light irradiation

The fluorescein-derived hydroxyl radical (˙OH) sensor aminophenyl fluorescein (APF) was synthesized as described in literature[7] and used as a turn-on sensor to visualize the ˙OH radicals production by the photosensitizers through the oxidation of the non-fluorescent APF, leading to the fluorescent product fluorescein.[8] A Varian Cary Eclipse fluorescence spectrometer was used to detect the fluorescence of the emerging fluorescein while using the following settings: excitation at 492 nm, collection of the emission at 525 nm, slit width: 2.5 nm for excitation and emission, averaging time: 1 second. The cuvette was kept at a constant temperature of 25 °C while stirring.

As a positive control, the Fenton's reagent was applied to oxidize the APF. For this purpose, a freshly prepared solution of 5 µM APF (from a stock solution of APF in DMF) and 300 µM ammonium iron(II) sulfate (FAS, from a stock solution of FAS in H_2O) in PBS (3 mL total volume) in a cuvette was used as a blank (Figure S7) and measured for 30 s to ensure no fluorescence signal is detectable at 525 nm. Then, after 30 s H_2O_2 was added during the measurement in a way that the final H_2O_2 concentration reached 300 µM and the solution was measured for another 30 s to visualize the increase in fluorescence, showing the reactivity of the synthesized APF towards the produced ˙OH radicals (Figure S7).

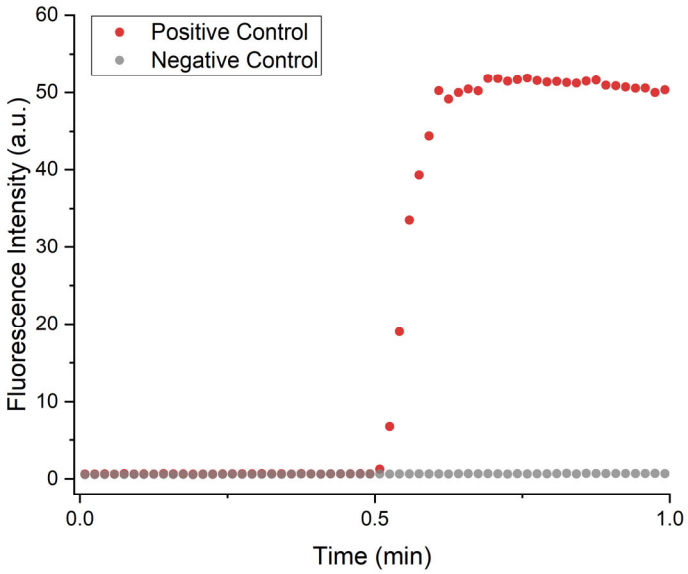

Figure S7. Positive and negative control experiments for the APF solution. An increase in fluorescence is detected once the Fenton's reagent produces ˙OH radicals in the positive control. No increase in fluorescence is detected in the negative control.

To show the generation of ˙OH radicals by **6**, **6-cPt** and **6-tPt** upon light irradiation, 1 mM stock solutions of **6**, **6-cPt** and **6-tPt** in MeOH were prepared. Then, 30 µL of each solution were 1000-fold diluted with 3 mL of a PBS solution containing 5 µM APF for every experiment, respectively. For every compound, the fluorescence intensity of the solution was measured at 525 nm for 1 min, before the cuvette was irradiated for another minute with light of 750 nm at a distance of 2 cm from the LED light source while stirring (light intensity at the distance applied: 1 mW/cm^2) and the fluorescence intensity measured again. This process was repeated until each solution was irradiated for 5 min in total. The mean and the standard deviation of the fluorescence signal for every measurement was determined and plotted below, showing the relative amount of ˙OH radicals produced by **6**, **6-cPt** and **6-tPt** (Figure S8). The rate of the ˙OH radical generation for the both platinated compounds **6-cPt** and **6-tPt** is 2-3-fold higher compared to the non-platinated species **6**.

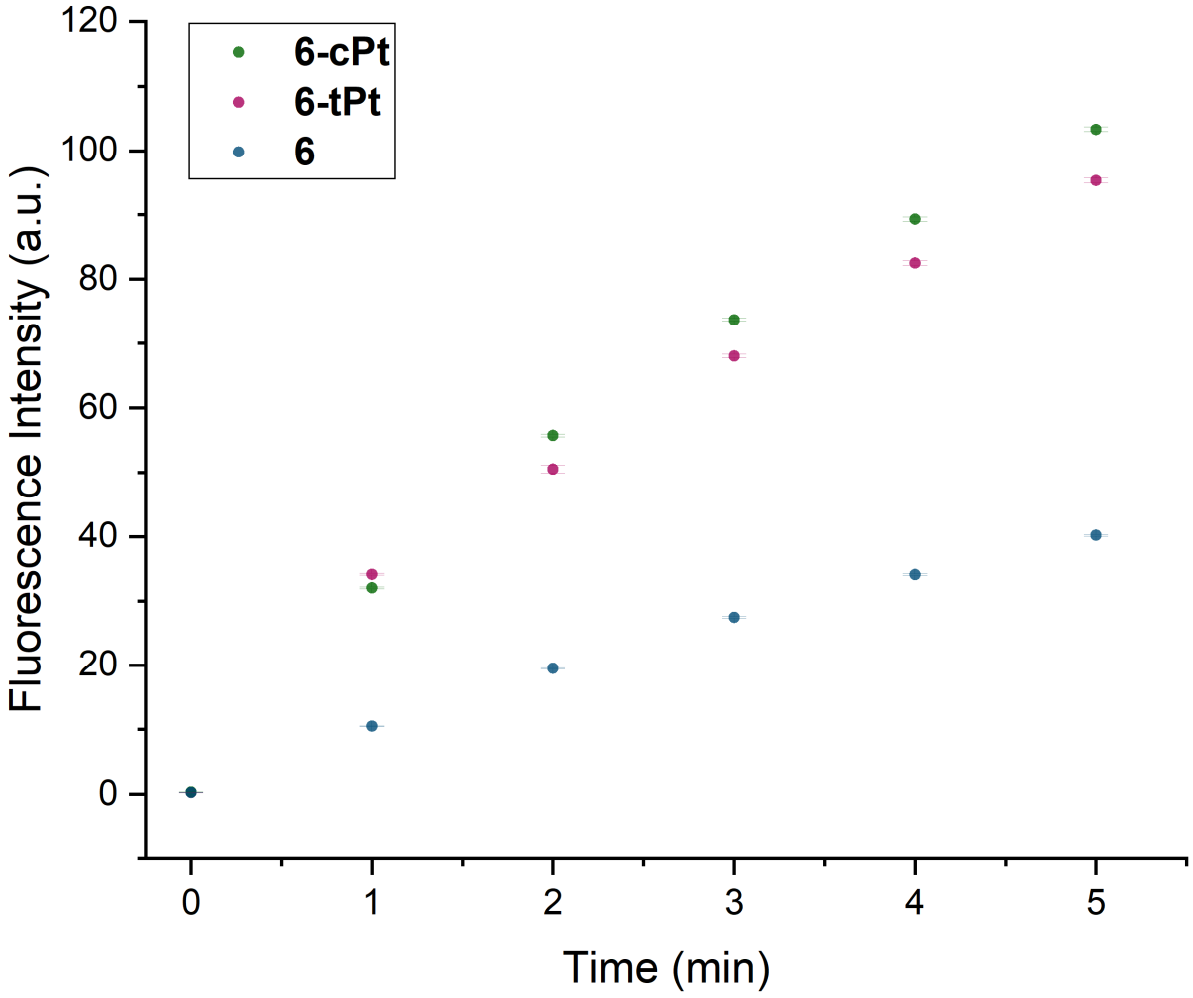

Figure S8. The relative rates of ˙OH radicals generation of **6** (blue), **6-cPt** (green) and **6-tPt** (purple) visualized through the emerging fluorescein.

Photodecomposition quantum yields

Photodecomposition quantum yields were determined using comparative method with ZnPc in DMSO as a standard ($\Phi_d = 2.51\times10^{-5}$)[9]. Solutions of photosensitizer (10 μM, 3 mL) in DMF (for BChls) or in DMSO (for ZnPc) were placed in the same cuvette holder with the temperature constantly controlled at 20°C. The solution was irradiated under constant stirring with the LED light sources with wavelengths of 760 nm and LED 690 nm for BChls and ZnPc respectively (the same light source system, cuvette holder with temperature control as describe above) (Figure S3). After every 15 min, the UV-Vis spectrum was recorded showing the photodecomposition of the PS.

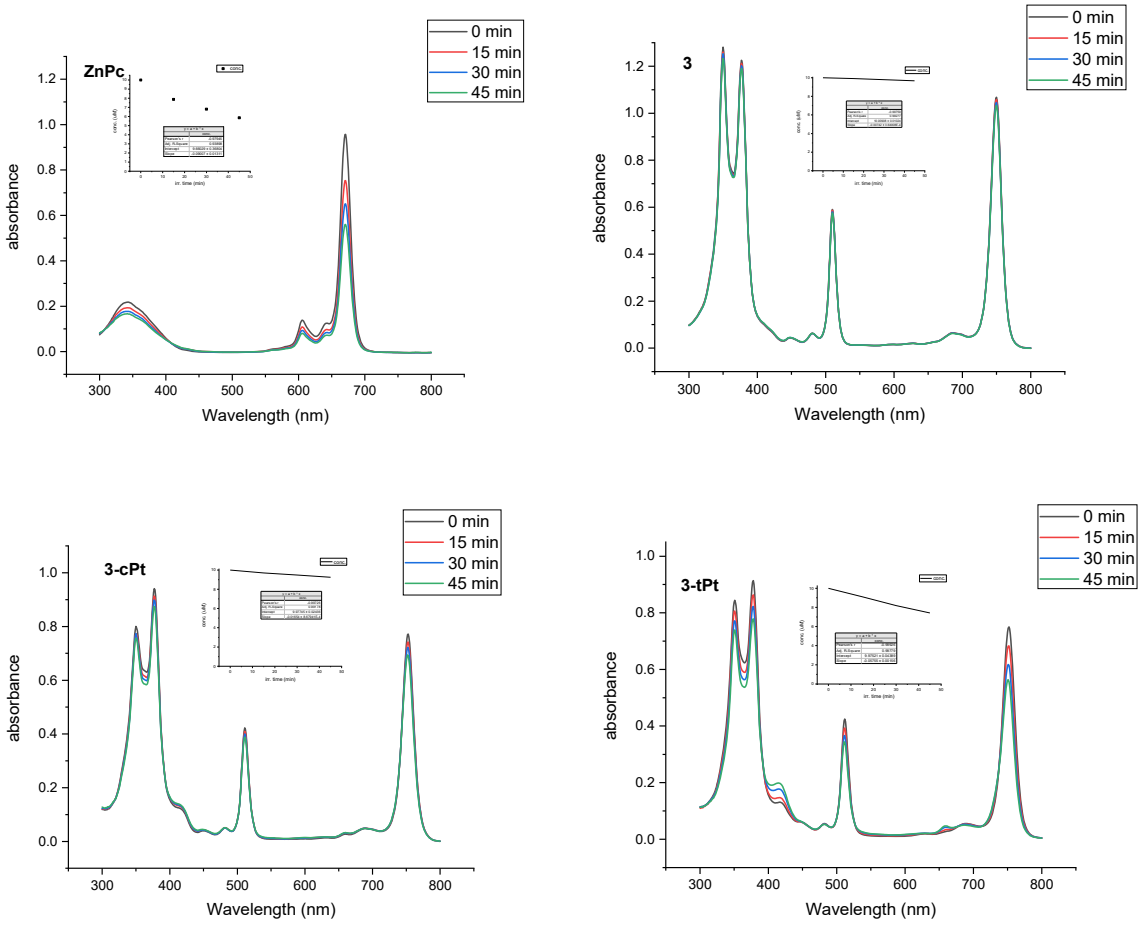

Figure S9. Photodecomposition of ZnPc and BChls **6**, **6-cPt** and **6-tPt** irradiated with LED light sources with wavelengths of 690 nm and 760 nm, respectively. UV-Vis spectra were recorded after every 15 min of irradiation. Inset: Plots of concentration of PS vs irradiation time.

In general, Φ_d is calculated as number of molecules decomposed divided by number of photons absorbed[9].

$$\Phi_d = \frac{\Delta N}{N_{photon}} = \frac{dC \times V \times N_A}{I_{(abs)} \times k \times S \times dt} \quad (5)$$

Where dC is the decrease in concentration over the period of time dt, V is the volume of the solution, N_A is Avogadro number, $I_{(abs)}$ is the rate of light absorption calculated as overlap of the LED irradiance spectra and the absorption spectra of the compound, calculated according to formula (3); k is the correction constant which characterizes for the relation between measured light irradiance intensity and the real values, S is the irradiated cell area.

Using the relative method by comparison with standard ZnPc, when the same volume and setup were used, leads to:

$$\Phi_{d(x)} = \Phi_{d(st)} \times \frac{\frac{dC_x}{dt} \times I_{abs(st)}}{\frac{dC_{st}}{dt} \times I_{abs(x)}} \quad (6)$$

The values of dC/dt could be derived from the plots of concentration of PS vs irradiation time, which showed the decrease of compound during irradiation.

Triplet state lifetimes and quantum yields

Triplet state lifetimes and quantum yields were measured with a LP920 Laser Flash Photolysis Spectrometer (Edinburgh Instruments) laser pump source: flashlamp pumped Q-switched Nd:YAG laser, probe source: xP920 pulsed xenon arc lamp, photomultiplier detector, oscilloscope Tektronix TDS3012C.

The transient absorption spectra were recorded in the range 300-900 nm after laser excitation λ = 355 nm (35 mJ/pulse and FWHM = 7 ns). Triplet state lifetimes were derived from kinetic curves at 780 nm with monoexponential fitting.

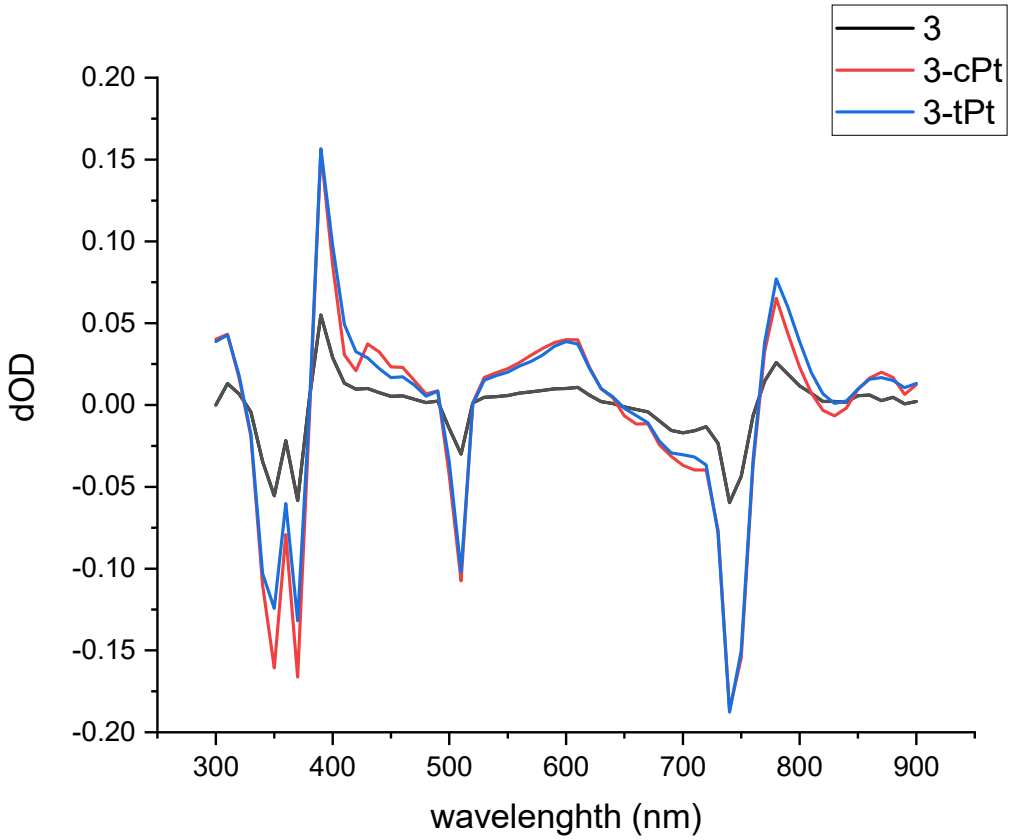

Figure S10. Transient absorption spectra of BChls **6**, **6-cPt** and **6-tPt** collected 10 ns after the laser pulse.

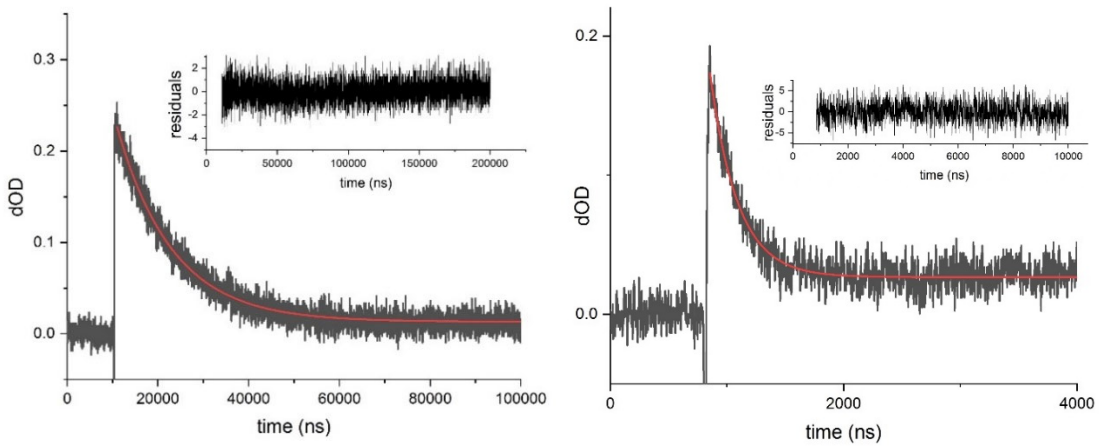

Figure S11. Decay of transient absorption of **6** at 780 nm under an atmosphere of N_2 (left) or air (right).

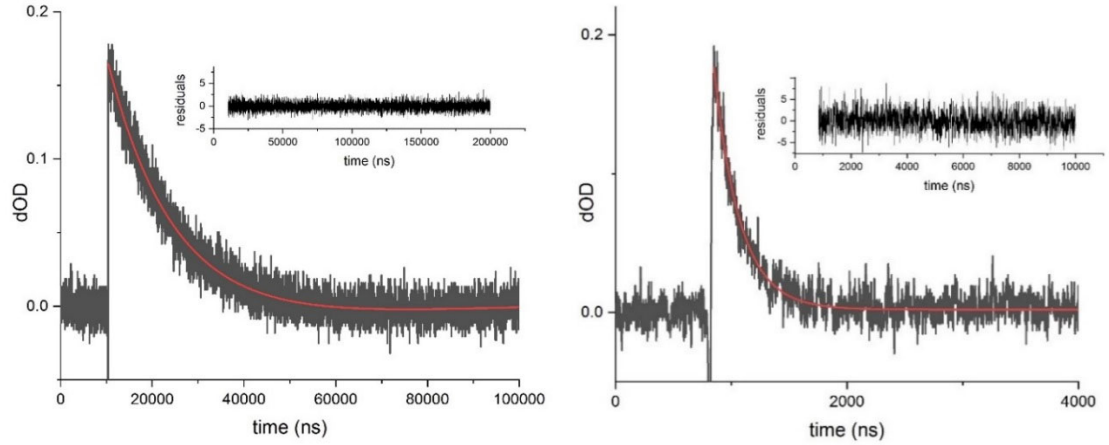

Figure S12. Decay of transient absorption of **6-cPt** at 780 nm under an atmosphere of N_2 (left) or air (right).

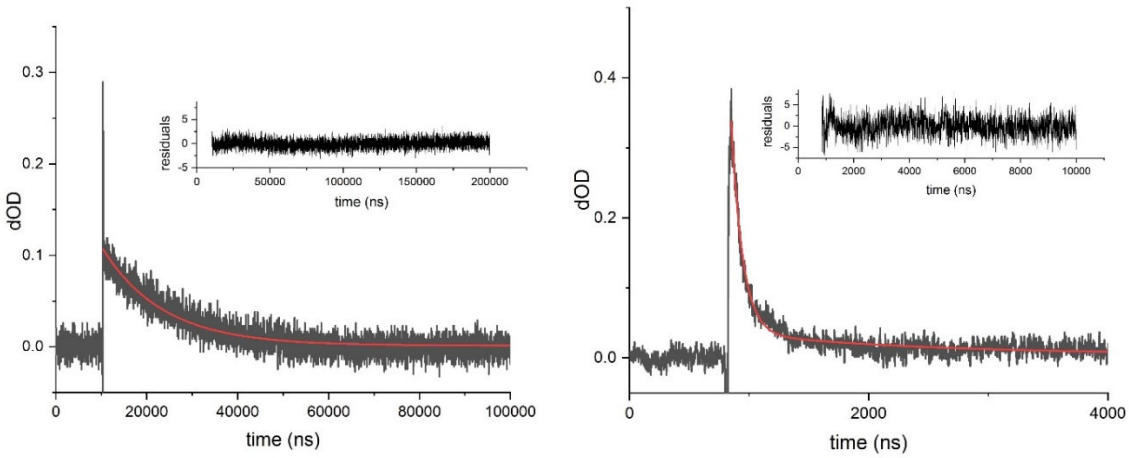

Figure S13. Decay of transient absorption of **6-tPt** at 780 nm under an atmosphere of N_2 (left) or air (right).

S4. Irradiation Setup for Cell Experiments

Cells were irradiated for the given amount of time stated in the description of the individual experiment with a LED light source (LED light source containing twelve LED750L LEDs, Thorlabs, USA mounted as an 3 x 4 LED array with distances of 2.8 cm between two LEDs on a 10 x 16 cm plate, constant current used = 150 mA) at a distance of 9.0 cm to the light source (light intensity: 1.40 mW/cm^2) in custom-built irradiation box containing a side fan to prevent possible cell death induced by heat accumulation due to the LED light source (Figure S14). No change of temperature was observed in the irradiation box during the measurements.

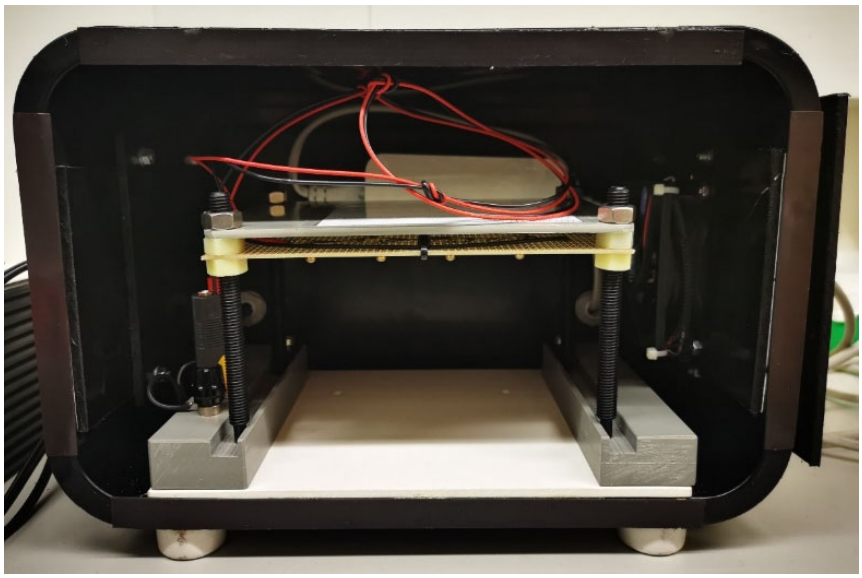

Figure S14. The custom-built irradiation box containing the LED light source.

S5. Photocytotoxicity

Human cervical carcinoma cells (HeLa) and non-cancerous MRC5 lung fibroblasts were cultured in DMEM (Gibco) supplemented with 5% fetal calf serum (Gibco), 100 U/mL penicillin, 100 µg/mL streptomycin. Ovarian cancer cell line A2780 were cultured in RPMI 1640 media supplemented with 2 mM Glutamine, 10% fetal calf serum, 100 U/mL penicillin, 100 µg/mL streptomycin. The cells were grown at 37 °C and under a humid atmosphere containing 5% CO_2. The cell lines were tested to be free of mycoplasm.

The photocytotoxicity of the PS compounds was evaluated using a resazurin-based fluorometric cell viability assay. Stock solutions of the PS (10 mM) were prepared in DMF and stored in the dark. 100 µL aliquots of cells in growth medium were seeded in 96-well plates (density of 4 × 10^3 cells/well) and incubated at 37 °C and 5% CO_2. After 24 h of incubation,

cells were treated with different concentrations (0.32 nM – 1 μM) of the test compounds and incubated for 4 h under light exclusion. Post 4 h, the growth medium containing the test compounds were replaced with fresh medium. For light irradiation, the cells were exposed to light at 750 nm for 60 min (corresponds to 5 J/cm^2) and allowed to grow for 72 h. For dark treatment, cells were treated similarly except for the light irradiation.

After 72 h incubation, the growth medium was replaced with 100 μL of freshly prepared resazurin containing growth medium (0.2 mg/mL final concentration), and cells were incubated at 37 °C for 4 h. Subsequently, fluorescence of the resorufin product (λ_{ex} = 540 nm) was quantified at 590 nm using a SpectraMax M5 microplate Reader. The reported cytotoxicity is the mean value of triplicate determinations for each drug concentration.

S6. Cellular Localization

Cellular localization of BChls was assessed by fluorescence confocal microscopy. HeLa cells were seeded with a density of 10^5 cells mL^{-1} on a μ-slide 8 wells ibiTreat plate (IBIDI, Germany, 300 μL per well) in DMEM (Gibco) supplemented with 5% fetal calf serum (FCS, Gibco) and 100 U mL^{-1} penicillin and 100 μg mL^{-1} streptomycin and were kept at 37 °C and 5% CO_2 for 24 h. Then, the cells were washed twice with warm PBS buffer and incubated for 3 h with 15 μM PS in DMEM with no FCS and 100 U mL^{-1} penicillin, 100 μg mL^{-1} streptomycin at 37 °C and 5% CO_2. 45 min prior imaging, Hoechst 33342 (10 μg mL^{-1}) and MitoTracker™ Green (200 nM), Golgi-ID® Green Assay Kit (100 μL per well, Enzo LifeSciences), ER-Tracker™ Green (1 μM, Invitrogen), LysoTracker™ (200 nM, Invitrogen) were added. The cells were washed twice with warm PBS buffer and the wells were filled with fresh medium (300 μL per well) without phenol red. The cells were imaged on a Leica SP8 inverse FALCON, equipped with a diode laser (405 nm) and a flexible white light laser source (470−670 nm). The PS was excited with 514 nm, its emission was measured at 730−800 nm; Hoechst was excited with 405 nm, its emission was measured at 415−500 nm, MitoTracker™ and Golgi-ID® were excited with 488 nm, their emission was recorded at 505−550 nm and ER-Tracker™ and Lyso-Tracker™ were excited with 504 nm and their emissions were measured at 514−550 nm. Cells stained with CellLight® Reagents BacMam 2.0 Mitochondria GFP were incubated 2 h after seeding with MitoBacMam solution (30 particles per cell, final concentration) for 22 h. MitoBacMam coupled with GFP was excited with 488 nm and its emission was recorded at 505−550 nm. Pictures were processed with Fiji ImageJ.

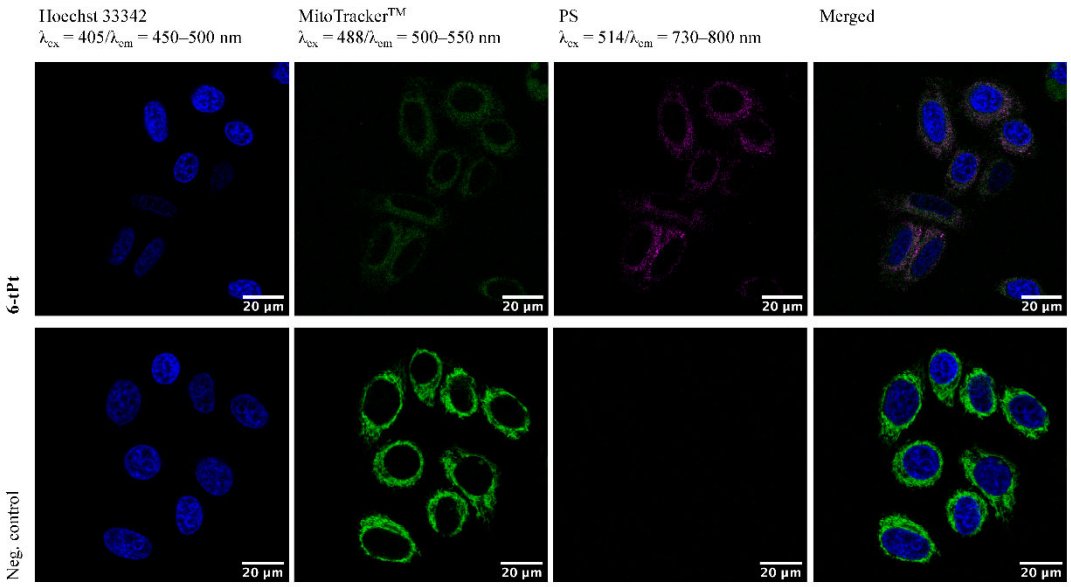

Figure S15. Cell localization with 15 µM of **6-tPt** and 200 nM of MitoTracker™ in HeLa cells. The fluorescence of the MitoTracker™ is significantly reduced by the applied PS **6-tPt**.

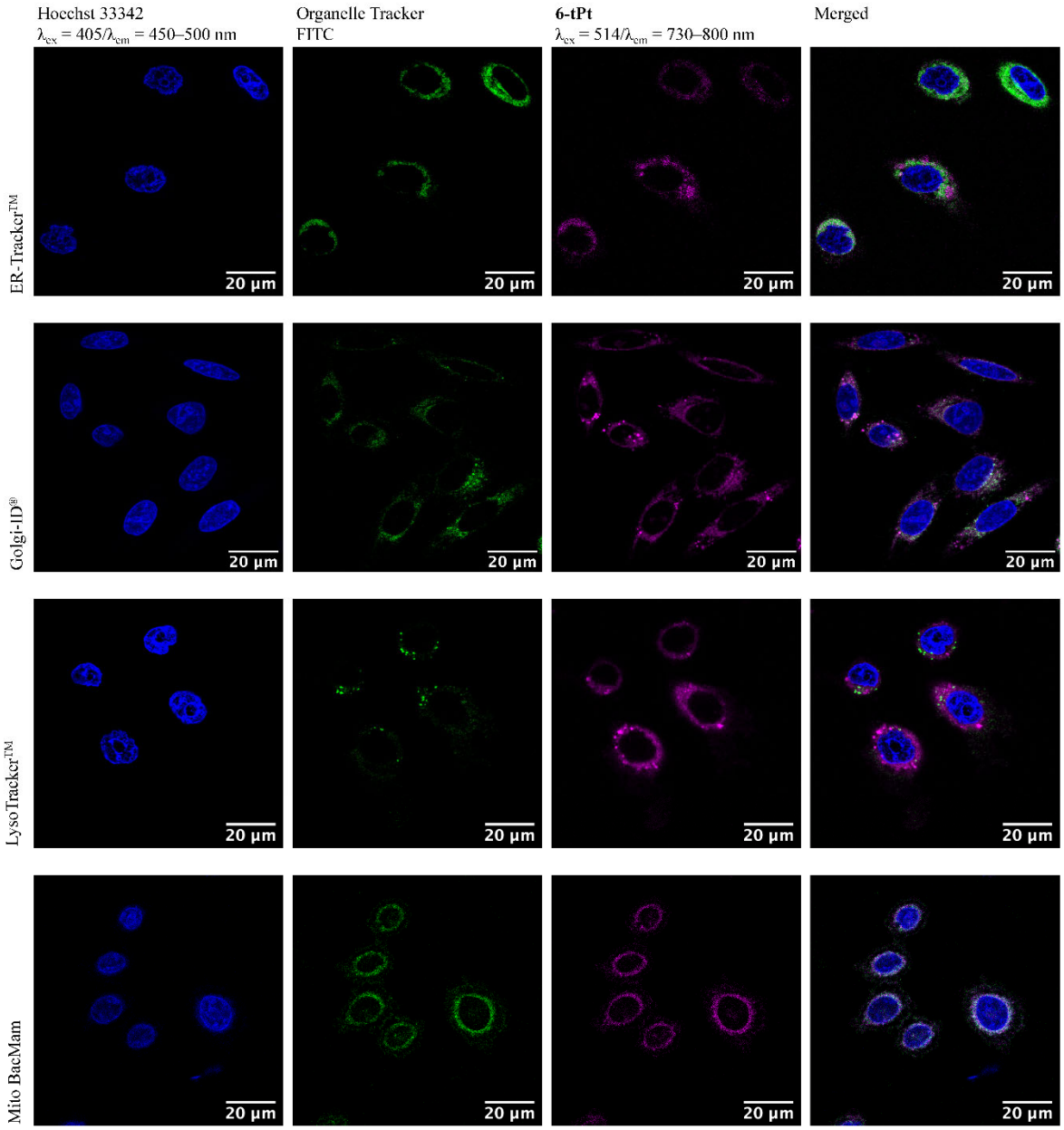

Figure S16. Cell localization with 15 µM of **6-tPt** and different compartment staining agents.

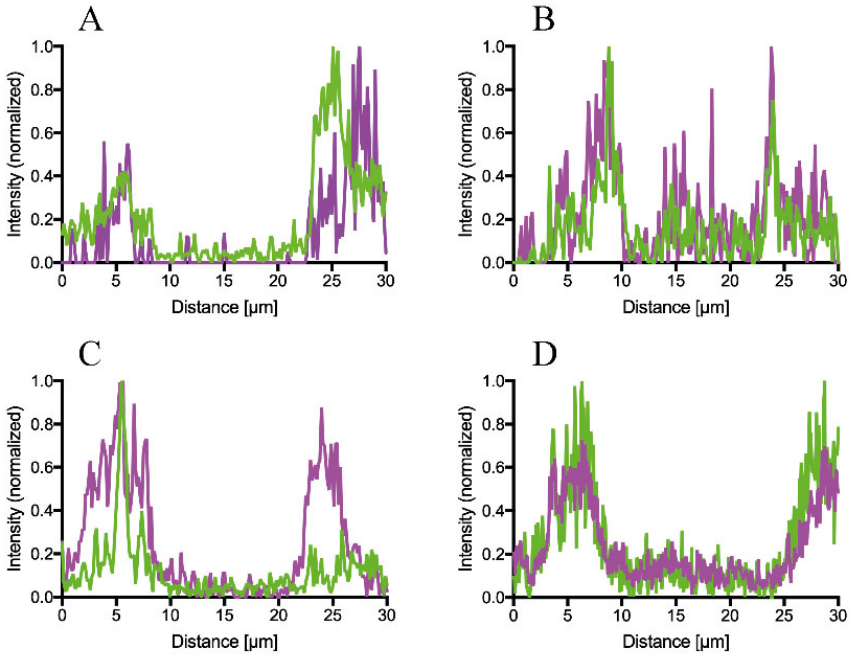

Figure S17. Normalized Intensities of the fluorescence of **6-tPt** (magenta) and the organelle dyes (green). The applied trackers are A) ER-Tracker™, B) Golgi-ID®, C) LysoTracker™ and D) Mito BacMam, respectively. Most overlap was found in mitochondria, and to a minor extend in ER.

S7. Mitochondrion membrane dysfunction imaging

Mitochondrion membrane dysfunction was measured using the mitochondrion membrane potential kit MAK147 from Sigma-Aldrich. HeLa cells were seeded at a density of 2 x 10^5 cells mL^{-1} in 35 mm glass bottom dish (1 mL per dish) in DMEM (Gibco), supplemented with 5% fetal calf serum (FCS, Gibco) and 100 U mL^{-1} penicillin and 100 µg mL^{-1} streptomycin, and were kept at 37 °C and 5% CO_2 for 24 h. The reagents were mixed following the manufacturer's instructions. The cells were incubated with the PS for 3 h with a concentration of 15 µM and 0.1 µM for the dark as well as the light sample and with the solution vector (15 µL MeOH) for the negative control. Before irradiation, the samples were all washed twice with warm PBS and supplemented with fresh media. The light samples were irradiated in our custom-made irradiation chamber for 30 min (750 nm, 2.5 J cm^{-2}), the dark and negative control were kept in the dark at rt and the positive control was incubated with 5 µM CCCP for 30 min at rt in the dark. Assay buffer A, with additionally 10 µg ml^{-1} Hoechst 33342 (final concentration) was then added and incubated for 15 min at rt. The cells were washed again once with PBS and incubated with assay buffer B for at least 10 min. Shortly before imaging, assay buffer B was removed, the cells were washed twice with PBS and 1 ml PBS was added to prevent the cells from drying out. The cells were imaged on a Leica SP8 inverse FALCON, equipped with a diode laser (405 nm) and a flexible white light laser source (470 – 670 nm). Hoechst 33342 was excited with 405 nm, its emission was measured at 450 – 500 nm; the mitochondrion membrane potential dye was excited with 540 nm, its emission was measured at 550 – 620 nm; and the PS was excited with 514 nm, its emission was measured at 700 – 800 nm. The pictures were processed using Fiji ImageJ.

S8. Detection of Intracellular ROS Levels

2 x 10^5 HeLa cells in 2 ml DMEM supplemented with 5% FBS were seeded on 60 mm dishes. The following day, cells were treated with 10 nM **6-tPt** for 4 hours. Following the incubation, cells were washed with PBS and the medium was subsequently replaced with 2 mL DMEM. Cells were irradiated with 750 nm light for 2.5 J/cm^2, as described for the photocytotoxicity assay. After irradiation, H_2DCF-DA was added to the samples to a final concentration of 50 µM and incubated for 45 min at 37 °C. Cells were washed twice with PBS and collected by trypsinisation. Cells were suspended in 1ml PBS containing 1% FBS. Samples were analysed on an Attune NxT Cytometer (Thermo Fisher Scientific) using BL1 channel (excitation 488

nm, emission 515 nm) to measure DCF fluorescence. Results are expressed as mean percentage of ROS-positive cells over total cell population, obtained from three independent experiments with a minimum of 100'000 cells analysed per condition. The error bars represent the standard deviation (S.D).

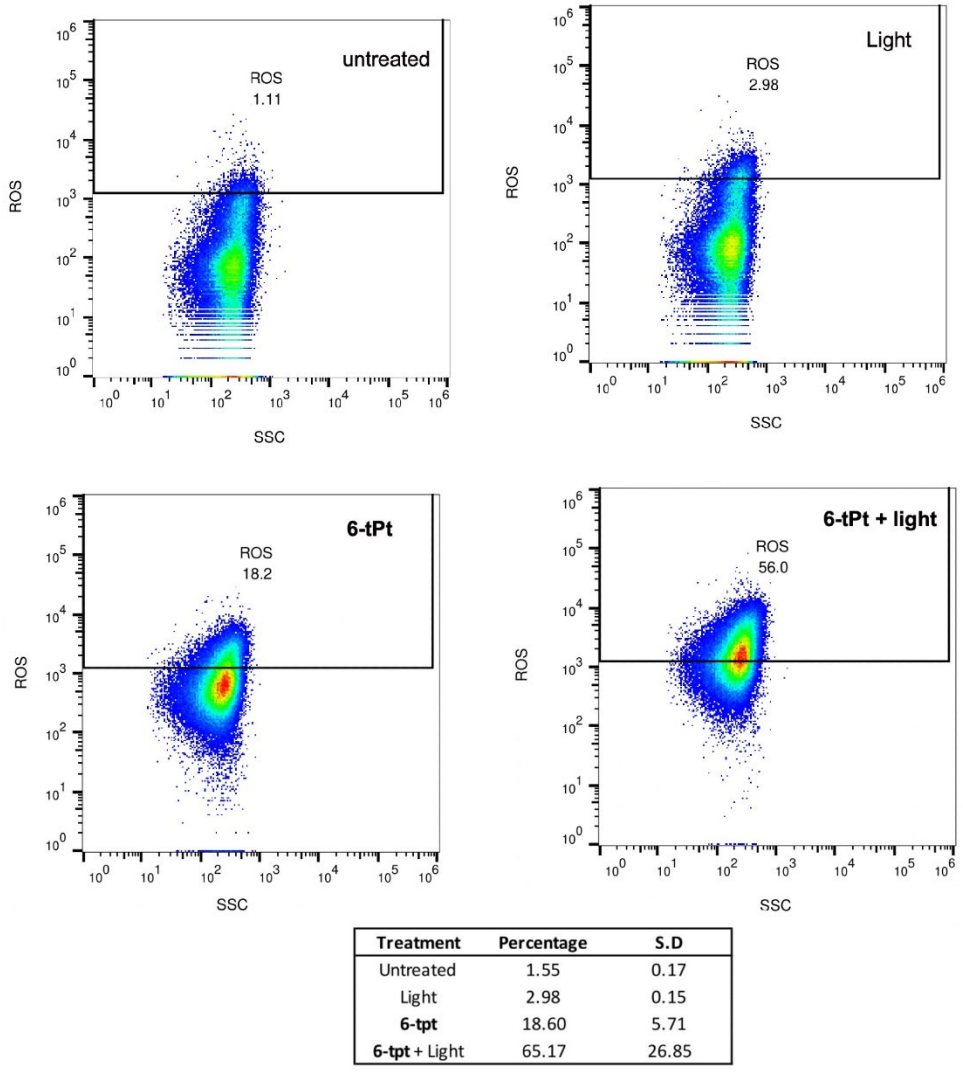

Treatment	Percentage	S.D
Untreated	1.55	0.17
Light	2.98	0.15
6-tpt	18.60	5.71
6-tpt + Light	65.17	26.85

Figure S18. Intracellular ROS production on HeLa cells treated with 10 nM of compound **6-tPt** for 4 h, irradiated at 750 nm light for 2.5 J/cm^2. ROS signal is indicated as the DCF fluorescence, measured using the BL1 channel (excitation 488 nm, emission 530 nm) on an Attune NxT. Cytometer and is plotted against side scatter (SSC). The median fluorescence intensity and the frequency of cells displaying ROS signal are shown.

S9. Table S2. Phototoxic properties of Bacteriochlorins against HeLa cells in the literature.

Normally only one compound with highest phototoxic index (PI) listed per paper or the lowest IC_{50} value.

Compound (together with compound number mentioned in the very reference)	**Light Source, λ and Light Dose**	**Photo-toxicity IC_{50} [μM]**	**Dark Toxicity IC_{50} [μM]**	**PI**	**Comments**	**Ref.**
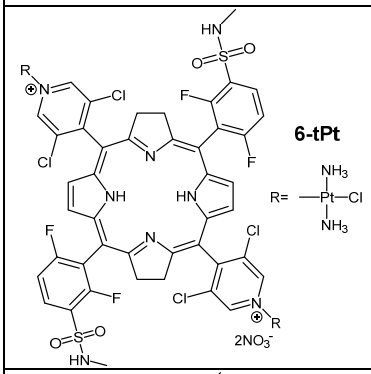 **6-tPt**	LED 750 nm 5 J/cm^2	0.011	44	4000	Stock solution in DMF	This work
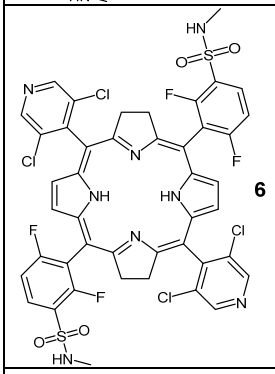 **6**	LED 750 nm 5 J/cm^2	0.21	124	590	Stock solution in DMF	This work
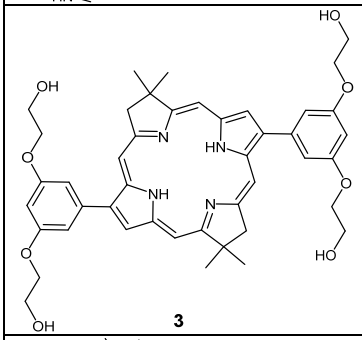 **3**	Laser 732 nm 10 J/cm^2	0.015	> 5	> 333		[10]
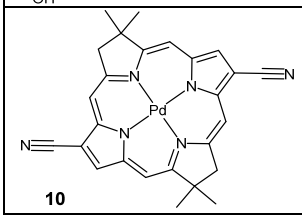 **10**	LED 760 nm 10 J/cm^2	0.025	> 5	> 200	Stock solution in DMA	[11]

S10. Table S3. Phototoxic properties of Chlorins against HeLa cells in the literature.

Normally only one compound with highest phototoxic index (PI) listed per paper or the lowest IC_{50} value.

Compound (together with compound number mentioned in the very reference)	**Light Source, λ and Light Dose**	**Phototoxicity IC_{50} [μM]**	**Dark Toxicity IC_{50} [μM]**	**PI**	**Comments**	**Ref.**
Fosan (*m*THPC) 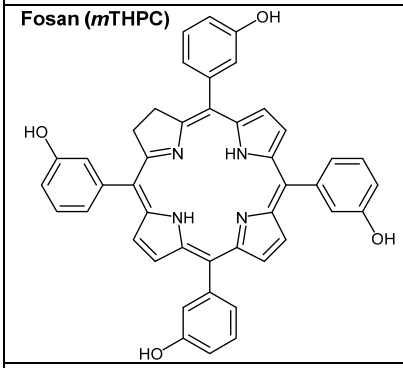	LED 637 nm 0.69 J/cm^2	0.38	Not known	Not known		12
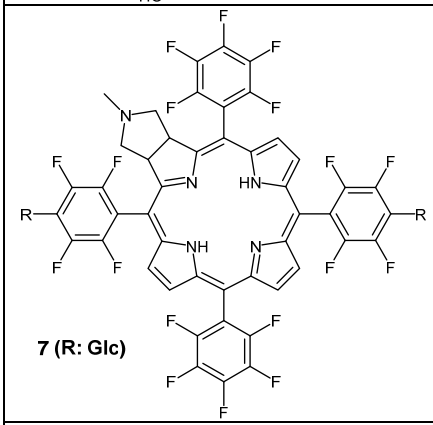 **7 (R: Glc)**	100 W Halogen lamp with 600 nm longpass filter 16 J/cm^2	0.0007	> 0.5	> 714	Max. relevant abs. at 656 nm	13
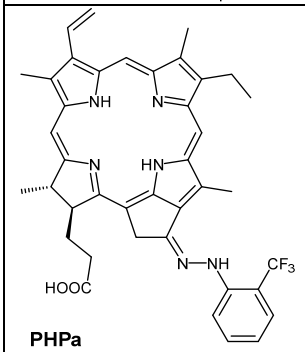 **PHPa**	irradiation with central λ at 675 nm 25 J/cm^2	1.9	> 120	> 63		14

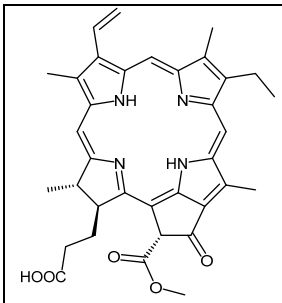 **Pheophorbide *a***	halogen lamp, 14 J/cm^2	0.15	>1	> 6.7	Max. relevant abs. at 668 nm[15]	16
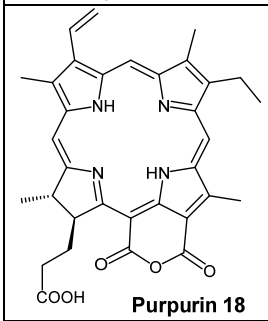 **Purpurin 18**	Laser 640 nm 8.6 J/cm^2	12	> 20	> 1.7		17
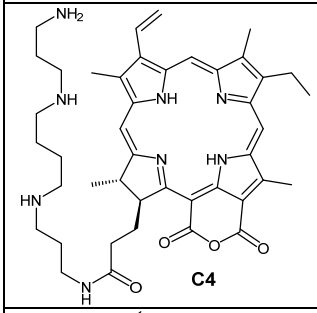 **C4**	Laser 640 nm 8.6 J/cm^2	1.8	> 20	> 11		17
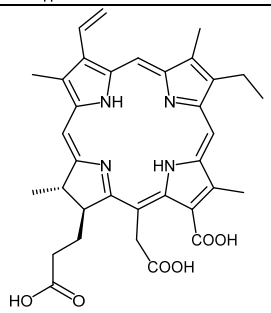 **e6**: main component of Radachlorin	LED 670 nm 27 J/cm^2	9.7	> 21	> 2.2		18

S11. Table S4. Light-dose dependence of the bacteriochlorins in HeLa cells.

Cells were incubated with the compounds for 4 h and then irradiated with varying light doses at 750 nm (1.25 J/cm^2 to 5 J/cm^2). Each of the independent experiments is an average value of triplicates.

Compound	**1.25 J/cm^2 (μM)** 15min 750nm	**2.5 J/cm^2 (μM)** 30min 750nm	**3.75 J/cm^2 (μM)** 45min 750nm	**5 J/cm^2 (μM)** 60min 750nm
6	>1	>1	0.436 ± 0.071	0.188 ± 0.001
6-cPt	0.117 ± 0.018	0.072 ± 0.012	0.058 ± 0.021	0.048 ± 0.033
6-tPt	0.037 ± 0.009	0.014 ± 0.013	0.011 ± 0.012	0.011 ± 0.003

S12. NMR spectra

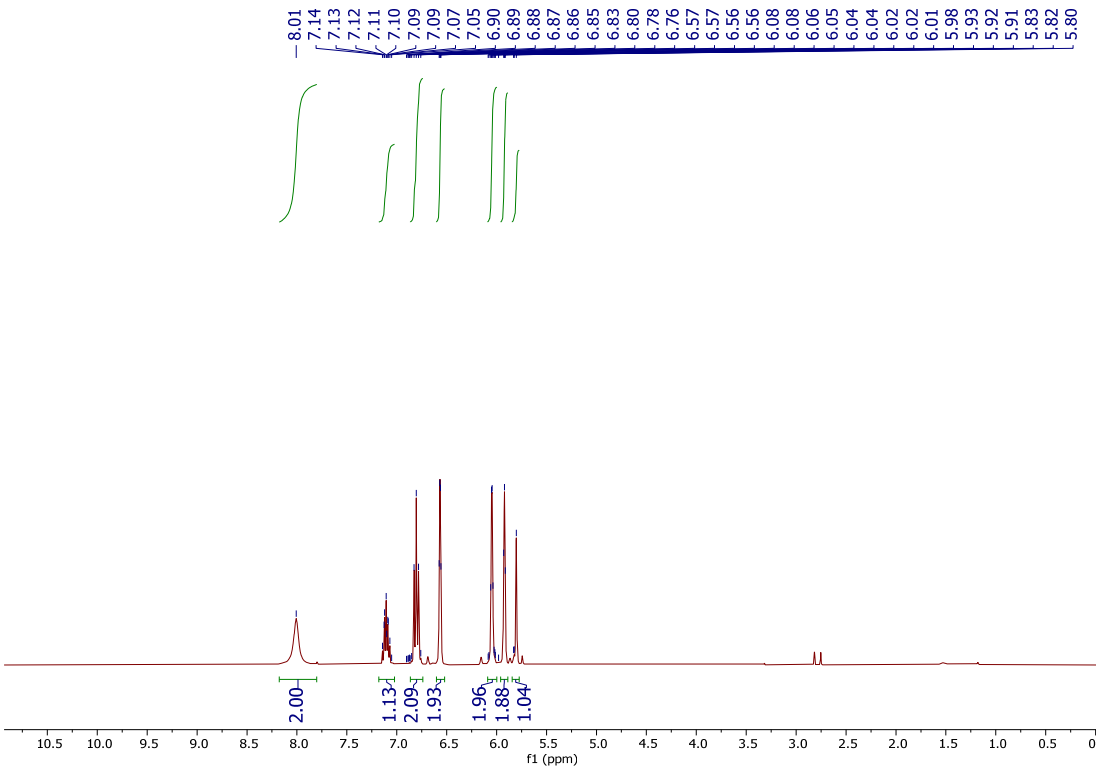

^{1}H-NMR of (2,6-difluorophenyl)dipyrromethane (**2**) in DMF-d$_7$

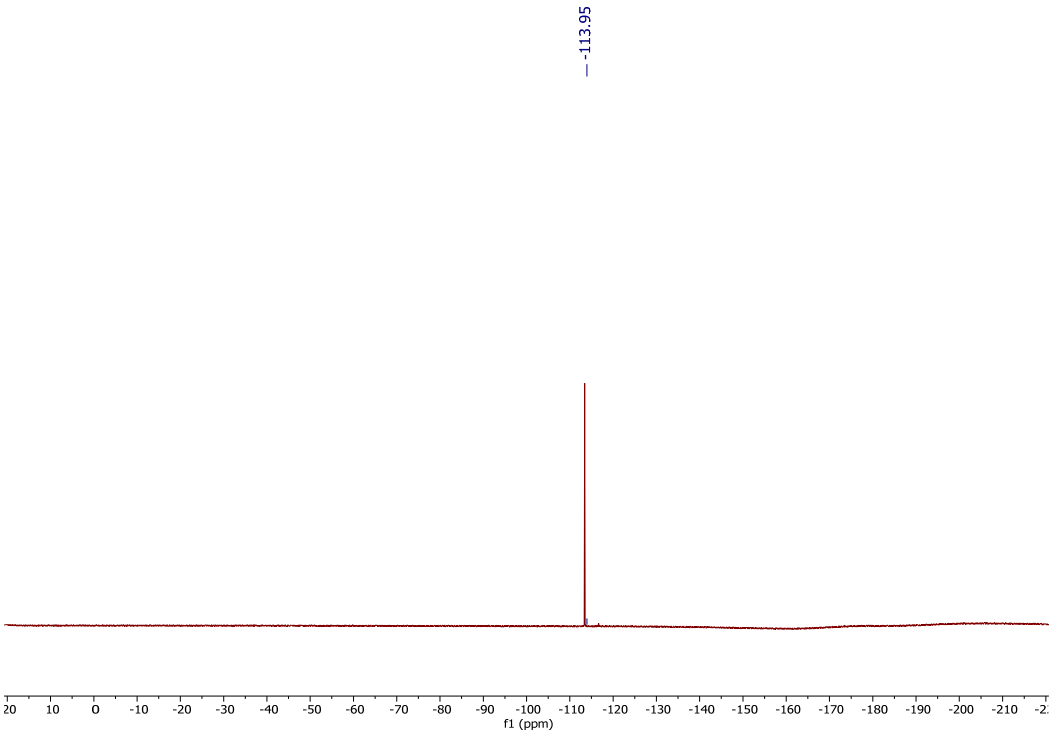

^{19}F-NMR of (2,6-difluorophenyl)dipyrromethane (**2**) in DMF-d$_7$

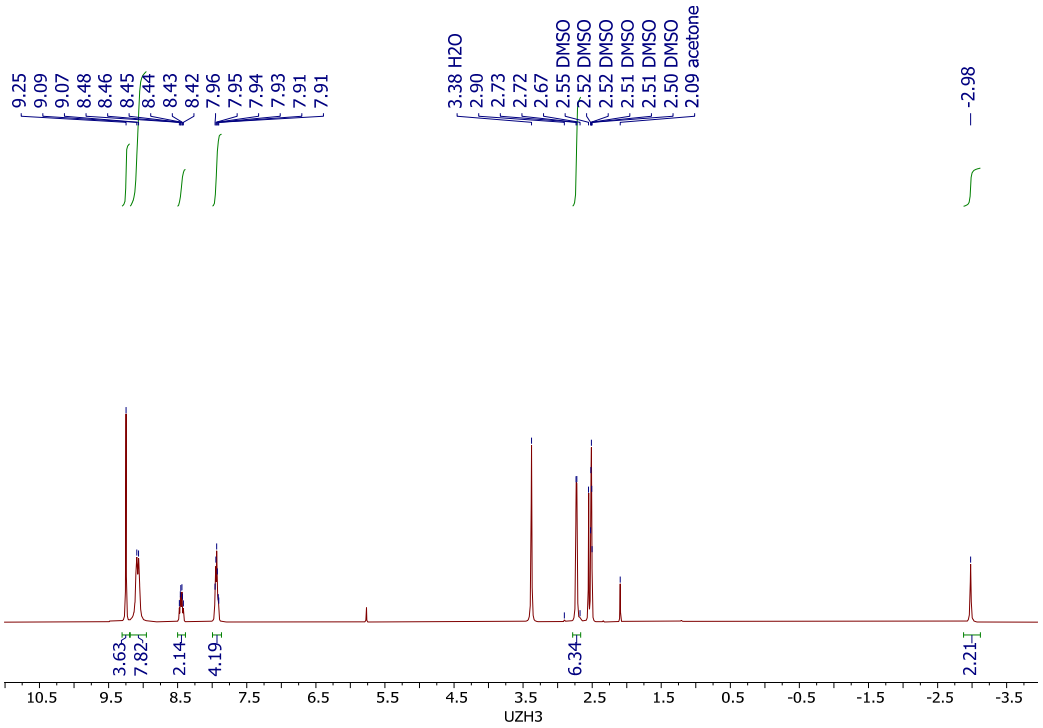

^{1}H-NMR of 5,15-bis(3,5-dichloropyridin-4-yl)-10,20-bis(2,6-difluoro-3-*N*-methylsulfamoylphenyl) porphyrin (**5**) in DMSO-d$_6$

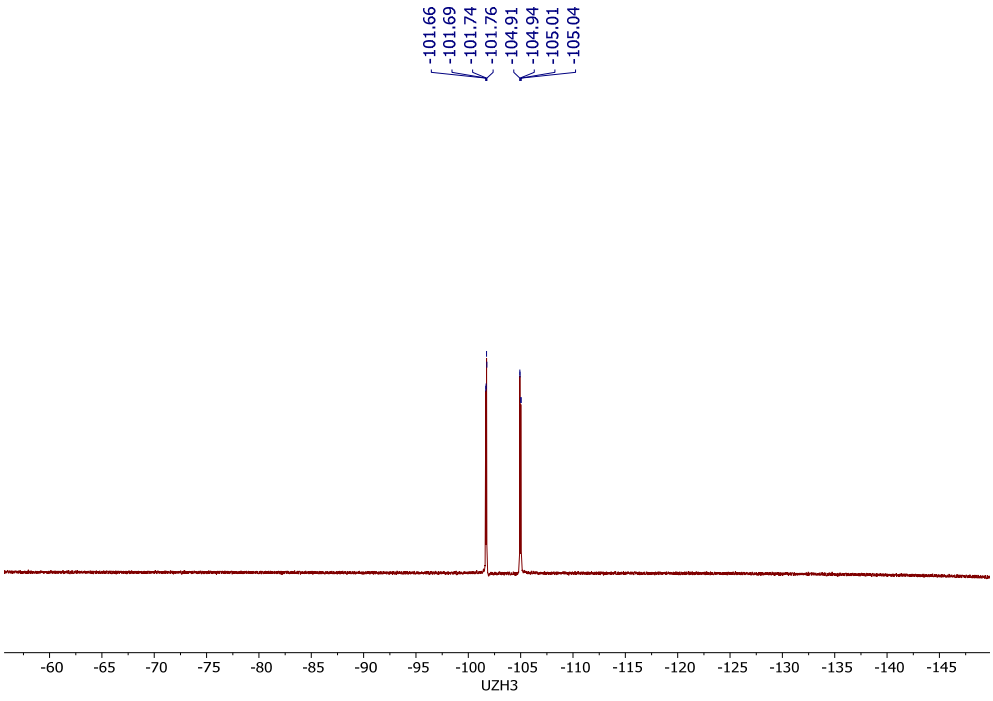

^{19}F-NMR of 5,15-bis(3,5-dichloropyridin-4-yl)-10,20-bis(2,6-difluoro-3-*N*-methylsulfamoylphenyl) porphyrin (**5**) in DMSO-d$_6$

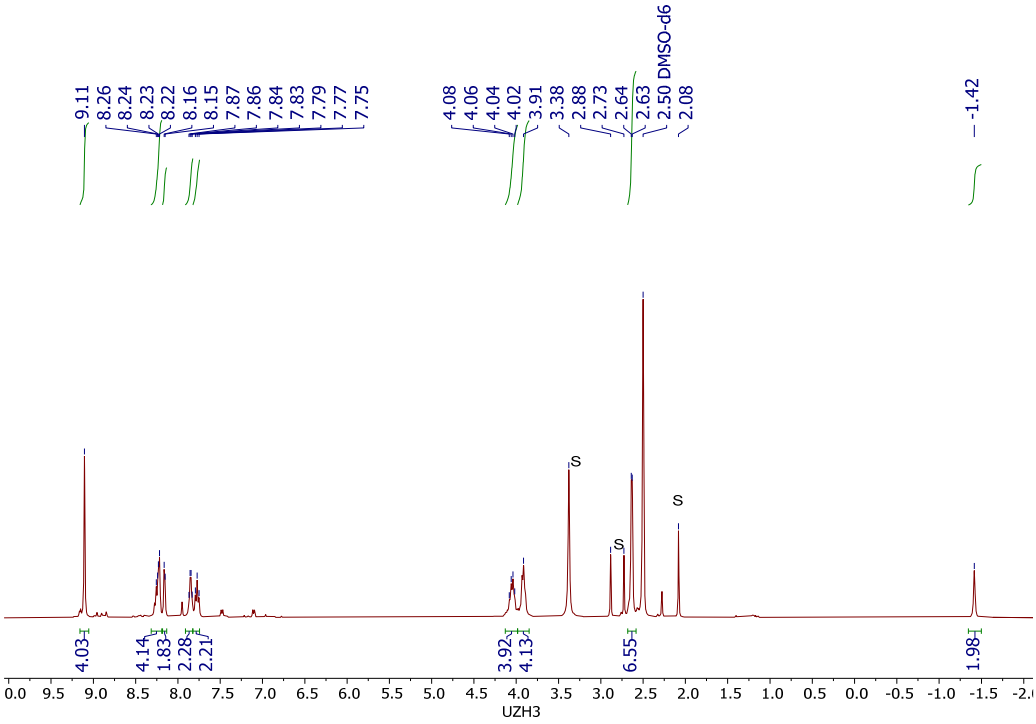

^{1}H-NMR of 5,15-bis(3,5-dichloropyridin-4-yl)-10,20-bis(2,6-difluoro-3-*N*-methylsulfamoylphenyl) bacteriochlorin (**6**) DMSO-d_6

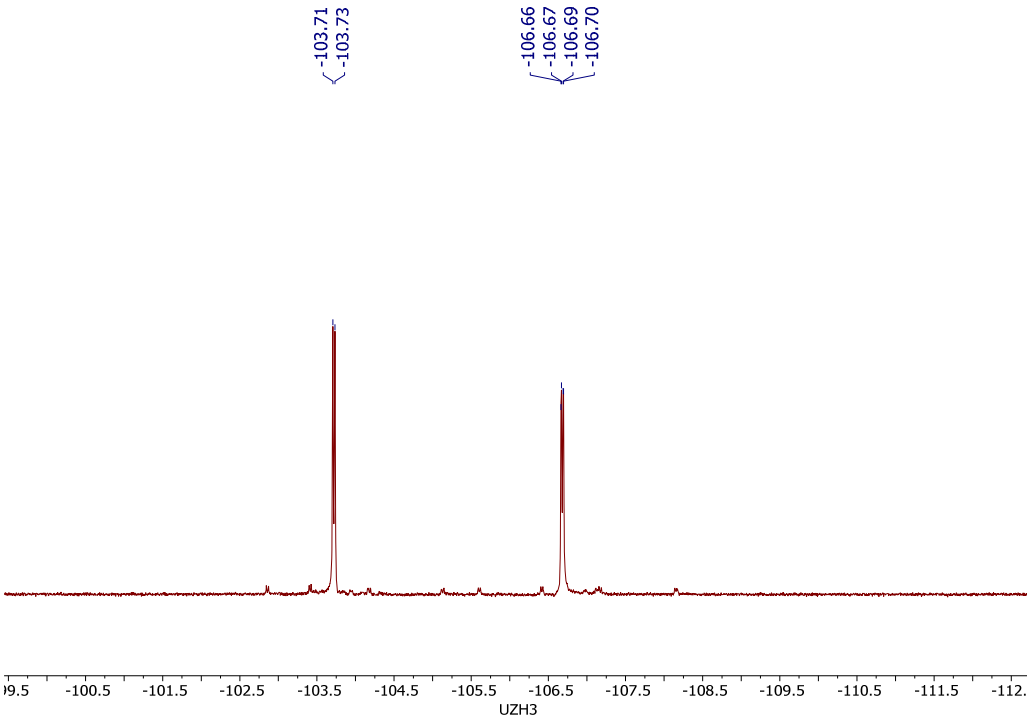

^{19}F-NMR of 5,15-bis(3,5-dichloropyridin-4-yl)-10,20-bis(2,6-difluoro-3-*N*-methylsulfamoylphenyl) bacteriochlorin (**6**) in DMF-d_7

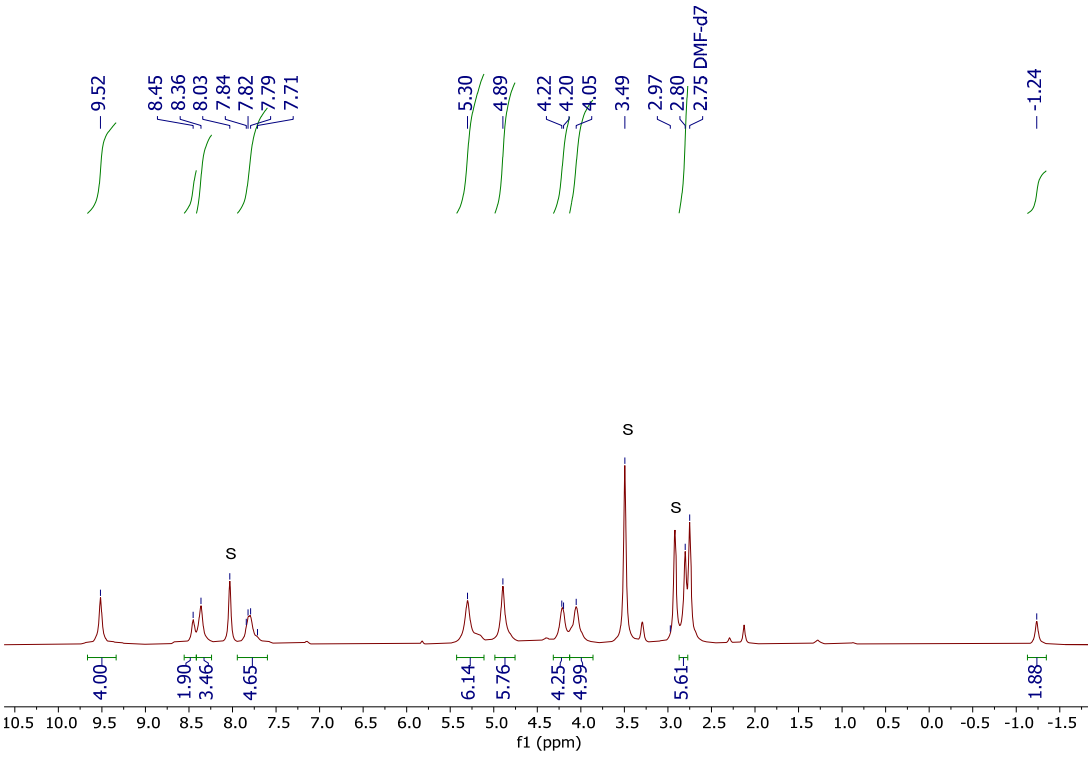

^{1}H-NMR of **6-cPt** in DMF-d_7

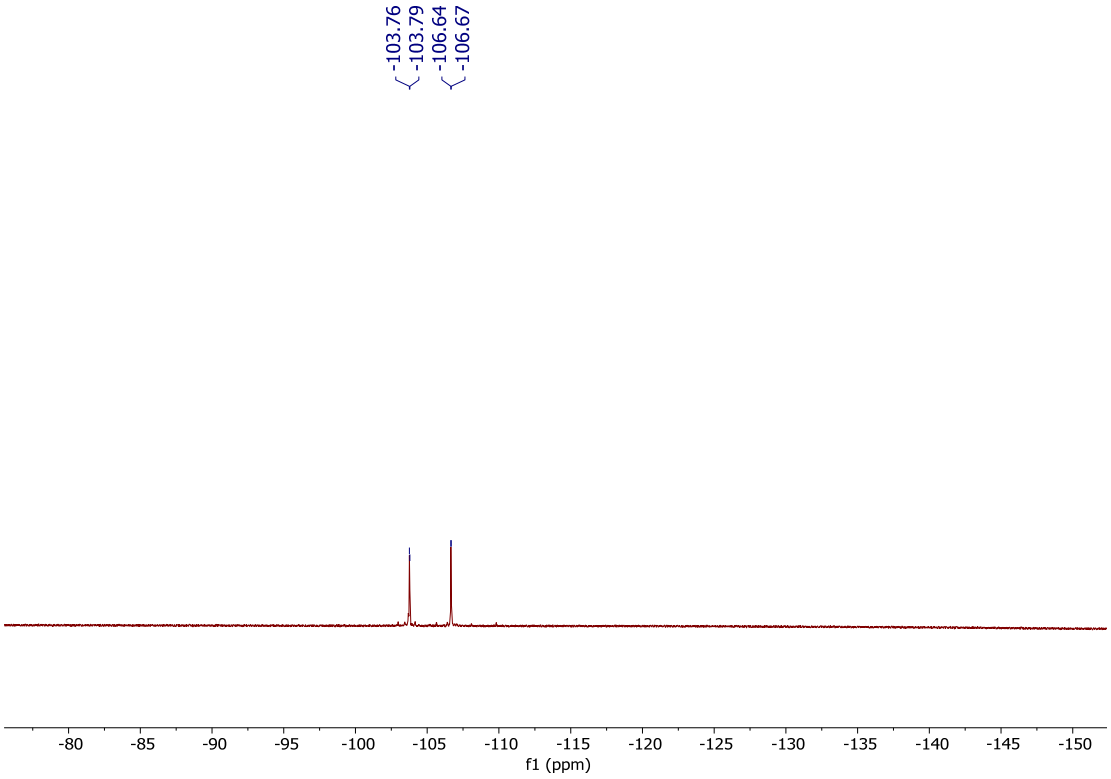

^{19}F-NMR of **6-cPt** in DMF-d_7

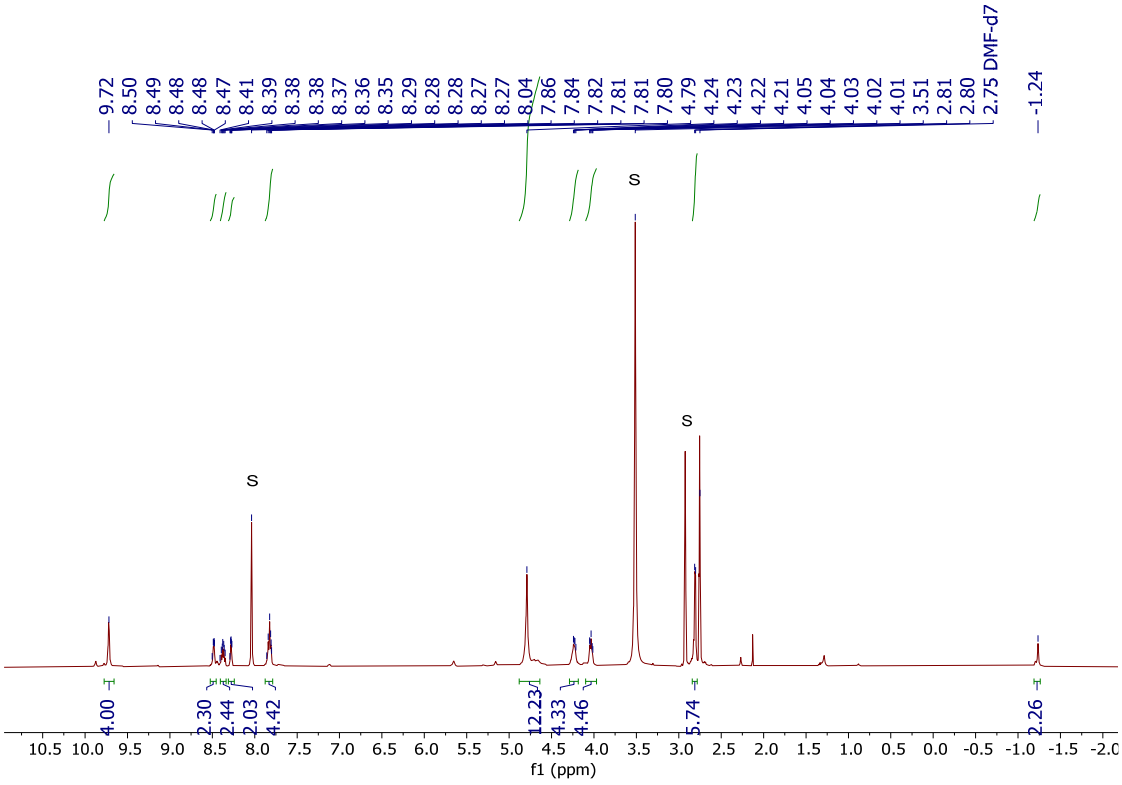

^{1}H-NMR of **6-tPt** in DMF-d$_7$

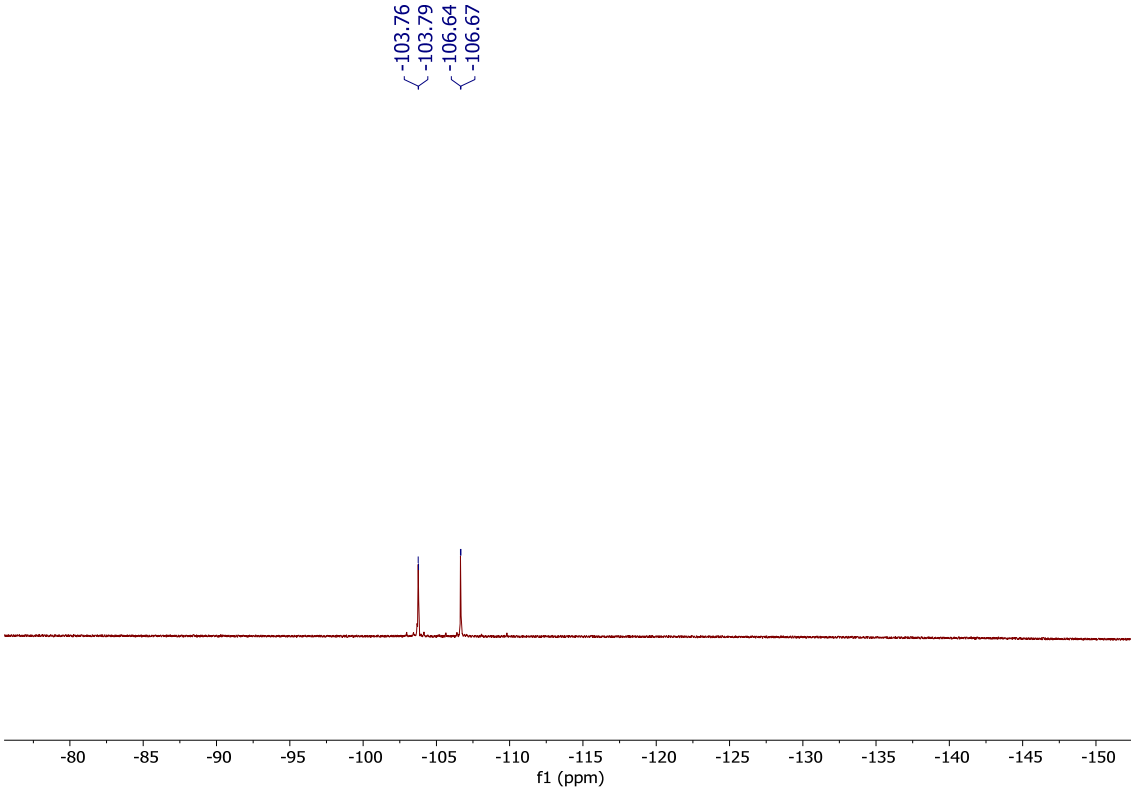

^{19}F-NMR of **6-tPt** in DMF-d$_7$

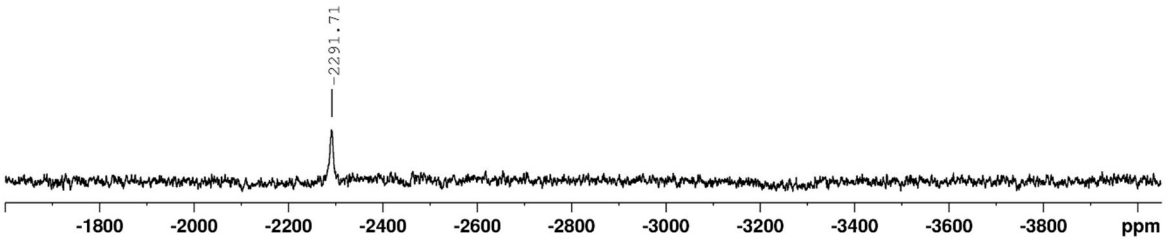

^{195}Pt-NMR of **6-cPt** in DMF-d_7

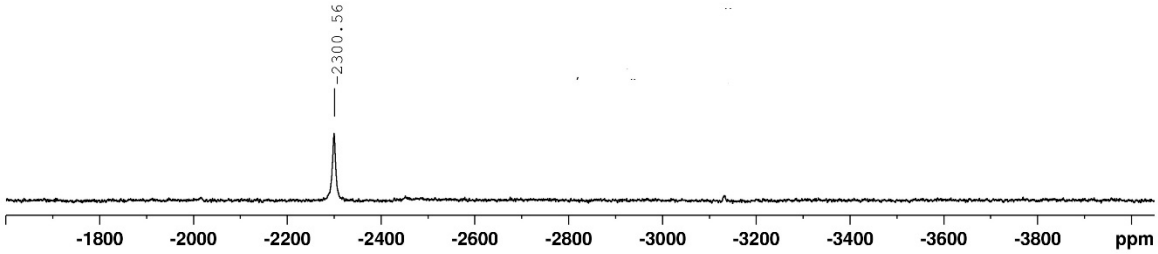

^{195}Pt-NMR of **6-tPt** in DMF-d_7

REFERENCES

(1) Miura, M.; Wu, H.: Symmetric and Asymmetric Halogen-Containing Metallocarboranylporphyrins and Uses Thereof, US8444953B2, 2013.

(2) Kopf, M.-A.; Karlin, K. D. Dioxygen Reactivity of Reduced Heme and Heme−Copper Complexes Utilizing Tetraarylporphyrinates Tethered with Both a Pyridyl Axial Ligand and N,N-Bis[2-(2-pyridyl)ethyl]amine Chelate. *Inorg. Chem.* **1999**, *38*, 4922-4923.

(3) Melhuish, W. H. Quantum efficiencies of fluorescence of organic substances: effect of solvent and concentration of the fluorescent solute. *J. Phys. Chem.* **1961**, *65*, 229-235.

(4) Williams, A. T. R.; Winfield, S. A.; Miller, J. N. Relative fluorescence quantum yields using a computer-controlled luminescence spectrometer. *Analyst* **1983**, *108*, 1067-1071.

(5) Schneider, L.; Larocca, M.; Wu, W.; Babu, V.; Padrutt, R.; Slyshkina, E.; König, C.; Ferrari, S.; Spingler, B. Exocyclically metallated tetrapyridinoporphyrazine as a potential photosensitizer for photodynamic therapy. *Photochem. Photobiol. Sci.* **2019**, *18*, 2792-2803.

(6) Tian, J.; Ding, L.; Xu, H.-J.; Shen, Z.; Ju, H.; Jia, L.; Bao, L.; Yu, J.-S. Cell-Specific and pH-Activatable Rubyrin-Loaded Nanoparticles for Highly Selective Near-Infrared Photodynamic Therapy against Cancer. *J. Am. Chem. Soc.* **2013**, *135*, 18850-18858.

(7) Liu, H.-Y.; Zhao, M.; Qiao, Q.-L.; Lang, H.-J.; Xu, J.-Z.; Xu, Z.-C. Fluorescein-derived fluorescent probe for cellular hydrogen sulfide imaging. *Chin. Chem. Lett.* **2014**, *25*, 1060-1064.

(8) Price, M.; Reiners, J. J.; Santiago, A. M.; Kessel, D. Monitoring Singlet Oxygen and Hydroxyl Radical Formation with Fluorescent Probes During Photodynamic Therapy. *Photochem. Photobiol.* **2009**, *85*, 1177-1181.

(9) Gürol, I.; Durmuş, M.; Ahsen, V.; Nyokong, T. Synthesis, photophysical and photochemical properties of substituted zinc phthalocyanines. *Dalton Trans.* **2007**, 3782-3791.

(10) Huang, Y.-Y.; Mroz, P.; Zhiyentayev, T.; Sharma, S. K.; Balasubramanian, T.; Ruzié, C.; Krayer, M.; Fan, D.; Borbas, K. E.; Yang, E.; Kee, H. L.; Kirmaier, C.; Diers, J. R.; Bocian, D. F.; Holten, D.; Lindsey, J. S.; Hamblin, M. R. In Vitro Photodynamic Therapy and Quantitative Structure-Activity

Relationship Studies with Stable Synthetic Near-Infrared-Absorbing Bacteriochlorin Photosensitizers. *J. Med. Chem.* **2010**, *53*, 4018-4027.

(11) Huang, Y.-Y.; Balasubramanian, T.; Yang, E.; Luo, D.; Diers, J. R.; Bocian, D. F.; Lindsey, J. S.; Holten, D.; Hamblin, M. R. Stable Synthetic Bacteriochlorins for Photodynamic Therapy: Role of Dicyano Peripheral Groups, Central Metal Substitution (2H, Zn, Pd), and Cremophor EL Delivery. *ChemMedChem* **2012**, *7*, 2155-2167.

(12) Etcheverry, M. E.; Pasquale, M. A.; Garavaglia, M. Photodynamic therapy of HeLa cell cultures by using LED or laser sources. *J. Photochem. Photobiol. B* **2016**, *160*, 271-277.

(13) Hirohara, S.; Oka, C.; Totani, M.; Obata, M.; Yuasa, J.; Ito, H.; Tamura, M.; Matsui, H.; Kakiuchi, K.; Kawai, T.; Kawaichi, M.; Tanihara, M. Synthesis, Photophysical Properties, and Biological Evaluation of *trans*-Bisthioglycosylated Tetrakis(fluorophenyl)chlorin for Photodynamic Therapy. *J. Med. Chem.* **2015**, *58*, 8658-8670.

(14) Cheng, J.; Li, W.; Tan, G.; Wang, Z.; Li, S.; Jin, Y. Synthesis and in vitro photodynamic therapy of chlorin derivative 13^1-*ortho*-trifluoromethyl-phenylhydrazone modified pyropheophorbide-a. *Biomed. Pharmacother.* **2017**, *87*, 263-273.

(15) Kotkowiak, M.; Dudkowiak, A. Multiwavelength excitation of photosensitizers interacting with gold nanoparticles and its impact on optical properties of their hybrid mixtures. *Phys. Chem. Chem. Phys.* **2015**, *17*, 27366-27372.

(16) Rapozzi, V.; Miculan, M.; Xodo, L. E. Evidence that photoactivated pheophorbide a causes in human cancer cells a photodynamic effect involving lipid peroxidation. *Cancer Biol. Ther.* **2009**, *8*, 1318-1327.

(17) Darmostuk, M.; Jurášek, M.; Lengyel, K.; Zelenka, J.; Rumlová, M.; Dražar, P.; Ruml, T. Conjugation of chlorins with spermine enhances phototoxicity to cancer cells *in vitro*. *J. Photochem. Photobiol. B* **2017**, *168*, 175-184.

(18) Biswas, R.; Mondal, A.; Chatterjee, S.; Ahn, J. C. Evaluation of synergistic effects of sulforaphene with photodynamic therapy in human cervical cancer cell line. *Lasers Med. Sci.* **2016**, *31*, 1675-1682.